Dynamic motion of the bow shock and the magnetopause observed by THEMIS spacecraft

H. Zhang,[1,2] Q.-G. Zong,[3] D. G. Sibeck,[2] T. A. Fritz,[1] J. P. McFadden,[4] K.-H. Glassmeier,[5] and D. Larson[4]

Received 25 June 2008; revised 28 October 2008; accepted 1 December 2008; published 31 January 2009.

[1] We present an observational study of the dynamic motion of the bow shock and the magnetopause and suggest that the dynamic motion of the bow shock is due to the interaction of an interplanetary shock with the Earth's bow shock. THEMIS B spacecraft crossed the magnetopause, a discontinuity and the bow shock successively in 5 min during its outbound journey on 10 July 2007. Following THEMIS B, THEMIS C, D, E and A consecutively crossed the magnetopause and the discontinuity but not the bow shock. Timing analysis shows that the magnetopause and the discontinuity were moving earthward with speeds of ~47 km/s and ~90 km/s, respectively. There is a trend that the discontinuity decelerates as it propagates toward the magnetopause. We suggest that the dynamic motion and the discontinuity are results of the interaction of a weak (M_A = 1.4) interplanetary shock with the Earth's bow shock. After the interaction, the transmitted interplanetary shock took the form of a discontinuity where total magnetic field and density increase and the temperature decreases. The rotation of the magnetic field across this discontinuity was similar to that of the interplanetary shock. The expected fast shock ahead of the discontinuity for shock-shock interaction was not observed.

Citation: Zhang, H., Q.-G. Zong, D. G. Sibeck, T. A. Fritz, J. P. McFadden, K.-H. Glassmeier, and D. Larson (2009), Dynamic motion of the bow shock and the magnetopause observed by THEMIS spacecraft, *J. Geophys. Res.*, *114*, A00C12, doi:10.1029/2008JA013488.

1. Introduction

[2] The Earth's bow shock is a fast mode magnetohydrodynamic (MHD) shock wave in front of the magnetopause which turns the supersonic solar wind flow into subsonic magnetosheath flow. The bow shock and the magnetopause move in response to changing upstream solar wind conditions [e.g., *Völk and Auer*, 1974; *Lepidi et al.*, 1996; *Maksimovic et al.*, 2003; *Glassmeier et al.*, 2008]. The speed of the bow shock motion ranges from tens to several hundreds of kilometers [e.g., *Greenstadt et al.*, 1972; *Guha et al.*, 1972; *Formisano et al.*, 1973; *Zastenker et al.*, 1988; *Maksimovic et al.*, 2003]. Dynamic pressure changes play a significant role in driving the bow shock motion although other parameters have effect too [e.g., *Spreiter et al.*, 1966; *Binsack and Vasyliunas*, 1968; *Wu et al.*, 1993]. On these time scales, the most significant solar wind features are tangential discontinuities [e.g., *Burlaga and Ogilvie*, 1969; *Sari and Ness*, 1969; *Burlaga*, 1971], interplanetary shocks [e.g., *Gosling et al.*, 1967, 1968; *Burlaga and Ogilvie*, 1969; *Ogilvie and Burlaga*, 1969] and Alfvén waves [e.g., *Belcher and Davis*, 1971]. Theoretical analysis shows that fast shock motion of the order of 100 km/s can be driven by interaction of tangential discontinuities or interplanetary shocks with the bow shock, while slow shock motion could be induced by small perturbation such as Alfvén waves [*Völk and Auer*, 1974].

[3] Both theoretical and observational efforts have been made to investigate the interaction of tangential discontinuities with the bow shock [*Völk and Auer*, 1974; *Formisano and Mastrantonio*, 1975; *Wu et al.*, 1993; *Maynard et al.*, 2007]. The interaction of a tangential discontinuity with the bow shock produces a new antisunward propagating fast shock ahead of the transmitted tangential discontinuity which has been observed [*Maynard et al.*, 2007]. The bow shock moves due to the dynamic pressure change across the discontinuity. The bow shock moves earthward (sunward) in the case of an enhanced (reduced) dynamic pressure behind the tangential discontinuity [*Wu et al.*, 1993].

[4] The interaction of interplanetary shocks with the bow shock has also been studied for a long time [e.g., *Shen and Dryer*, 1972; *Grib et al.*, 1979; *Zhuang et al.*, 1981; *Samsonov et al.*, 2006, 2007]. The interaction of an interplanetary shock with the bow shock launches a fast shock into the magnetosheath and forms a new discontinuity [*Zhuang et al.*, 1981]

[1]Center for Space Physics, Boston University, Boston, Massachusetts, USA.
[2]NASA Goddard Space Flight Center, Greenbelt, Maryland, USA.
[3]Center for Atmospheric Research, University of Massachusetts Lowell, Lowell, Massachusetts, USA.
[4]Space Sciences Laboratory, University of California, Berkeley, California, USA.
[5]Institute for Geophysics and Extraterrestrial Physics, Technical University of Braunschweig, Braunschweig, Germany.

0148-0227/09/2008JA013488

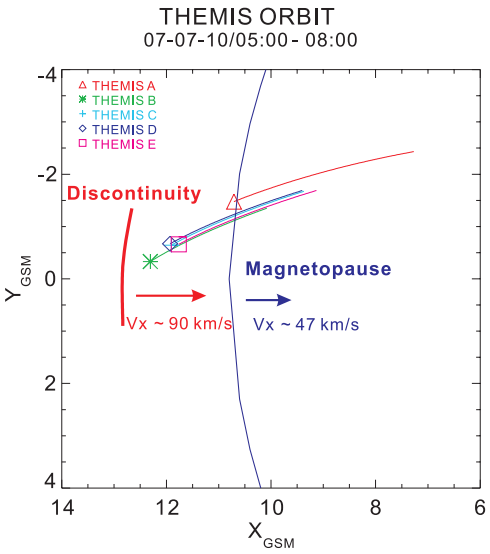

Figure 1. THEMIS trajectory projected in GSM XY plane from 0500 UT to 0800 UT on 10 July 2007. Timing analysis shows that both the magnetopause and the discontinuity are moving earthward. The velocities in X direction are ~47 km/s and ~90 km/s, respectively.

where the magnetic field strength and density increase, the temperature decreases and the velocity remains unchanged [*Samsonov et al.*, 2006]. This new discontinuity has been observed [*Šafránková et al.*, 2007; *Přech et al.*, 2008]. The bow shock moves earthward immediately after the interplanetary shock crossing [*Samsonov et al.*, 2006; *Přech et al.*, 2008]. Global MHD simulations show that the transmitted fast shock reflects from the inner numerical boundary and the bow shock and the magnetopause move sunward when the reflected shock passes [*Samsonov et al.*, 2007]. Earthward followed by sunward motion of the bow shock due to the interaction of an interplanetary shock with the bow shock has been observed [e.g., *Šafránková et al.*, 2007].

[5] *Koval et al.* [2006] studied the propagation of interplanetary shocks through the solar wind and the magnetosheath. They demonstrated that low Mach number interplanetary shocks may evolve on their way to the Earth.

[6] In this paper, we present THEMIS observations of the dynamic motion of the bow shock and the magnetopause and suggest that the motion of the bow shock is produced by the interaction of a weak interplanetary shock (M_A = 1.4) with the bow shock. After the interaction, the transmitted interplanetary shock took the form of a discontinuity where total magnetic field and density increase and the tempera-

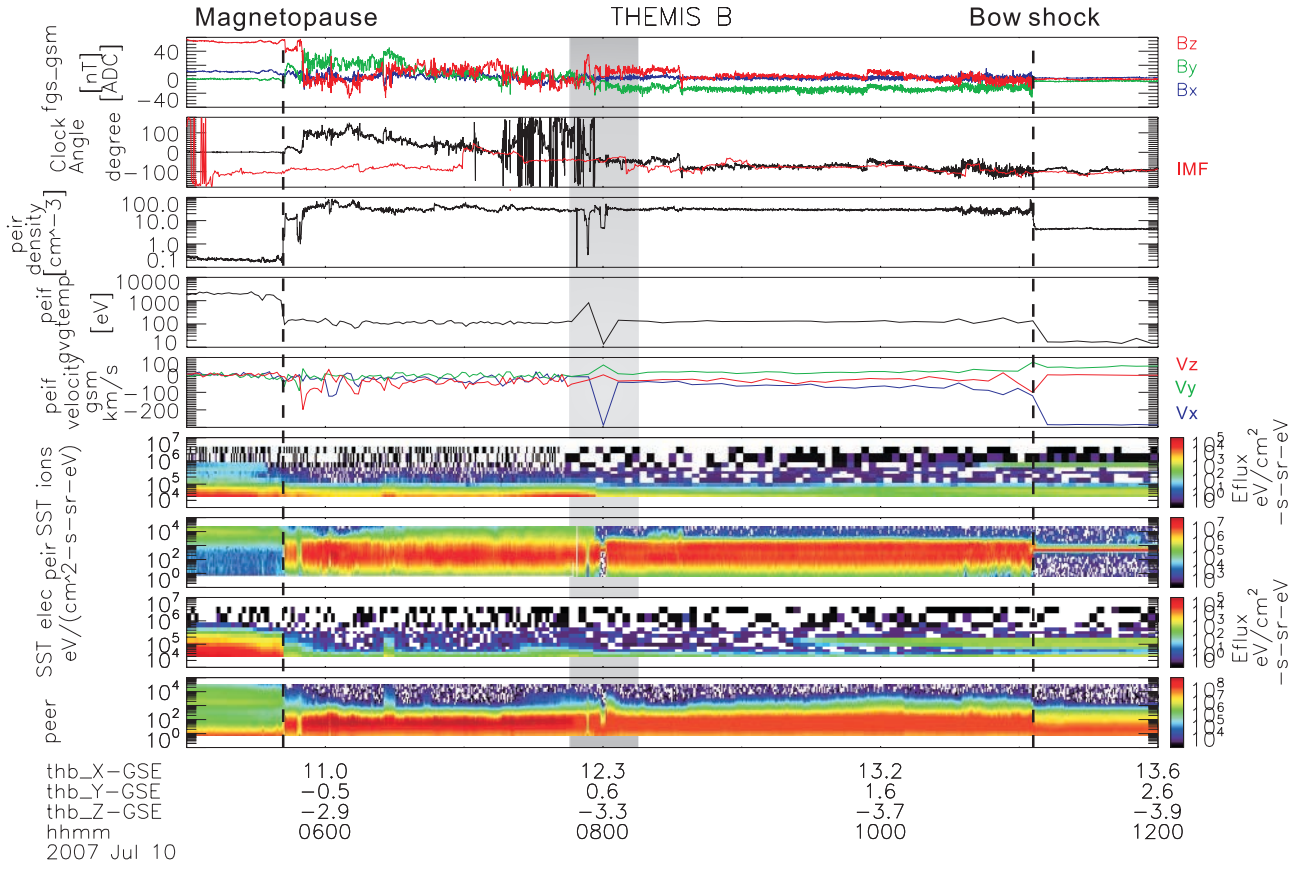

Figure 2. An overview plot of THEMIS B observations. From the top the panels show the following: components of the magnetic field in GSM coordinate system, clock angles of the magnetic field observed by THEMIS B (black line) and ACE spacecraft (red line, shifted 82 min for its convection to the Earth), plasma ion density, temperature, components of plasma flow, energetic ion (>30 keV) spectrum, plasma ion spectrum, energetic (>30 keV) electron spectrum and plasma electron spectrum. The vertical dashed lines at 0550 UT and 1106 UT mark the magnetopause and the bow shock, respectively. The shaded region is seen with greater time resolution in Figure 3.

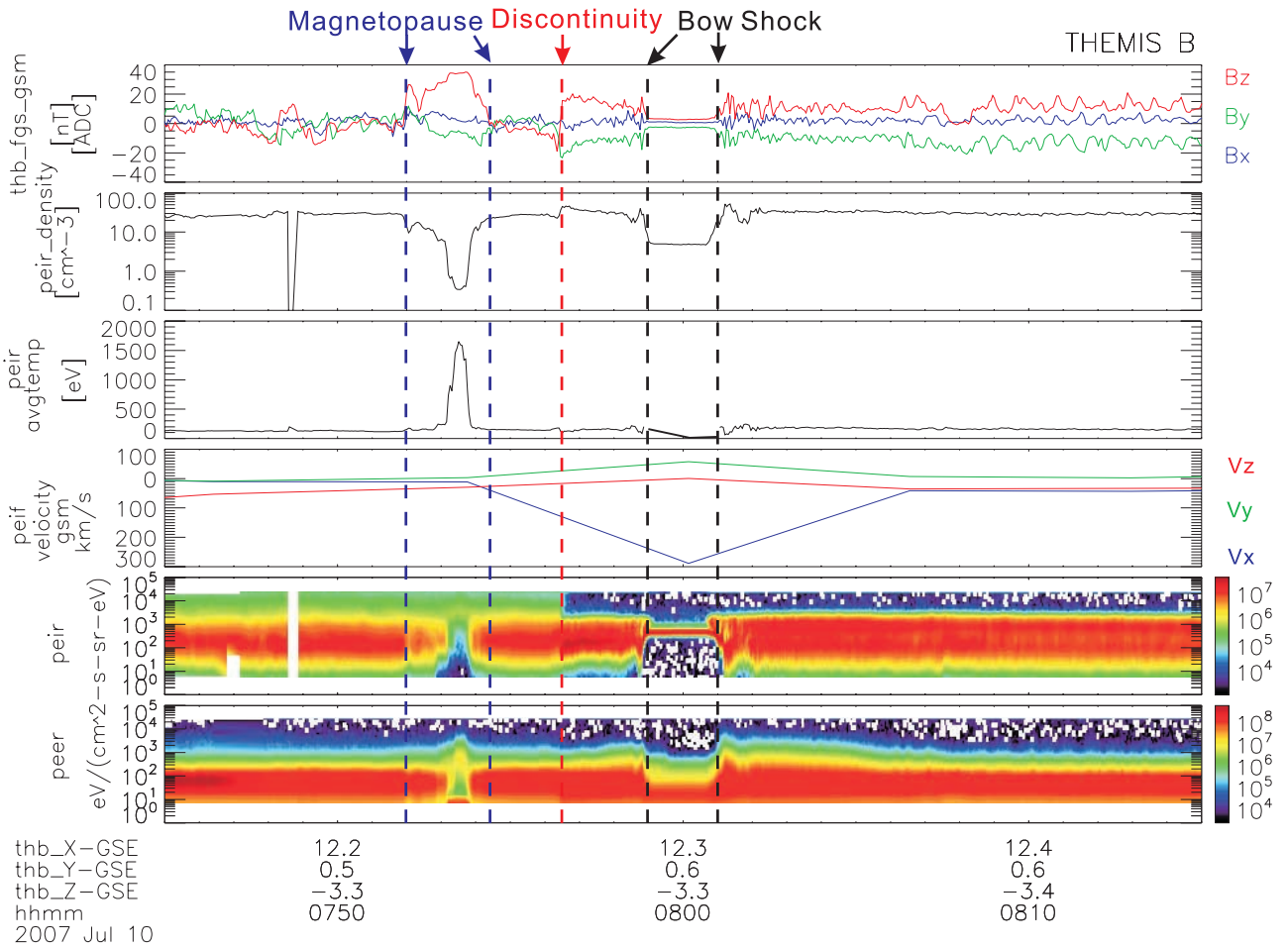

Figure 3. An overview plot of THEMIS B observations of the magnetopause, discontinuity and bow shock crossings. From the top the panels show the following: components of the magnetic field in GSM coordinate system, plasma ion density, temperature, components of plasma flow, plasma ion spectrum and plasma electron spectrum. The vertical blue, red and black dashed lines mark the magnetopause, the discontinuity and the bow shock crossings, respectively.

ture decreases. The rotation of the magnetic field across this discontinuity was similar to that of the interplanetary shock. The expected fast shock ahead of the discontinuity for shock-shock interaction was not observed.

2. Observations

[7] Figure 1 shows the trajectory of the THEMIS spacecraft [*Angelopoulos*, 2008] during its outbound journey from 0500 UT to 0800 UT on 10 July 2007. The positions of 5 THEMIS probes at 0800 UT are marked by five different symbols in Figure 1. THEMIS B was leading on this outbound pass and was followed by THEMIS C, D, E, and A. THEMIS C and D are very close to each other.

[8] Figure 2 gives an overview of the THEMIS spacecraft probe B observations of the magnetopause and bow shock crossings during its outbound journey on 10 July 2007. The first panel shows three components of the magnetic field in GSM coordinate system measured by FGM [*Auster et al.*, 2008]. The second panel shows the clock angles. The black line represents THEMIS observation and the red line represents the clock angle of the interplanetary magnetic field (IMF) observed by ACE Magnetic Field Experiment [*Smith et al.*, 1998]. The IMF data has been shifted 82 min for its convection to the Earth using the observed solar wind velocity by ACE. From 0835 UT to 1200 UT, these two clock angles agree well with each other indicating that ACE is a good solar wind monitor for that time period and 82 min time shift is reasonable. The following three panels show the plasma ion density, temperature and components of the plasma flow obtained by ESA instrument [*McFadden et al.*, 2008]. The last four panels show SST energetic ion (>30 keV) spectrum, ESA plasma ion spectrum, SST energetic (>30 keV) electron spectrum and ESA plasma electron spectrum. The magnetopause crossing at 0550 UT (marked by a vertical dashed line) is clearly identified by the sharp changes in the magnetic field, plasma ion density, temperature, velocity, plasma ion and electron spectra. The plasma in the magnetosphere is hot ($T \sim 2$ keV) and

Table 1. Normal Directions of the Magnetopause

UT	Normal Direction (GSE)	Method
05:50	(0.980,−0.103,−0.169)	MVA
07:52	(0.996,−0.080,−0.044)	MVA
07:54	(0.985,−0.077,−0.153)	MVA

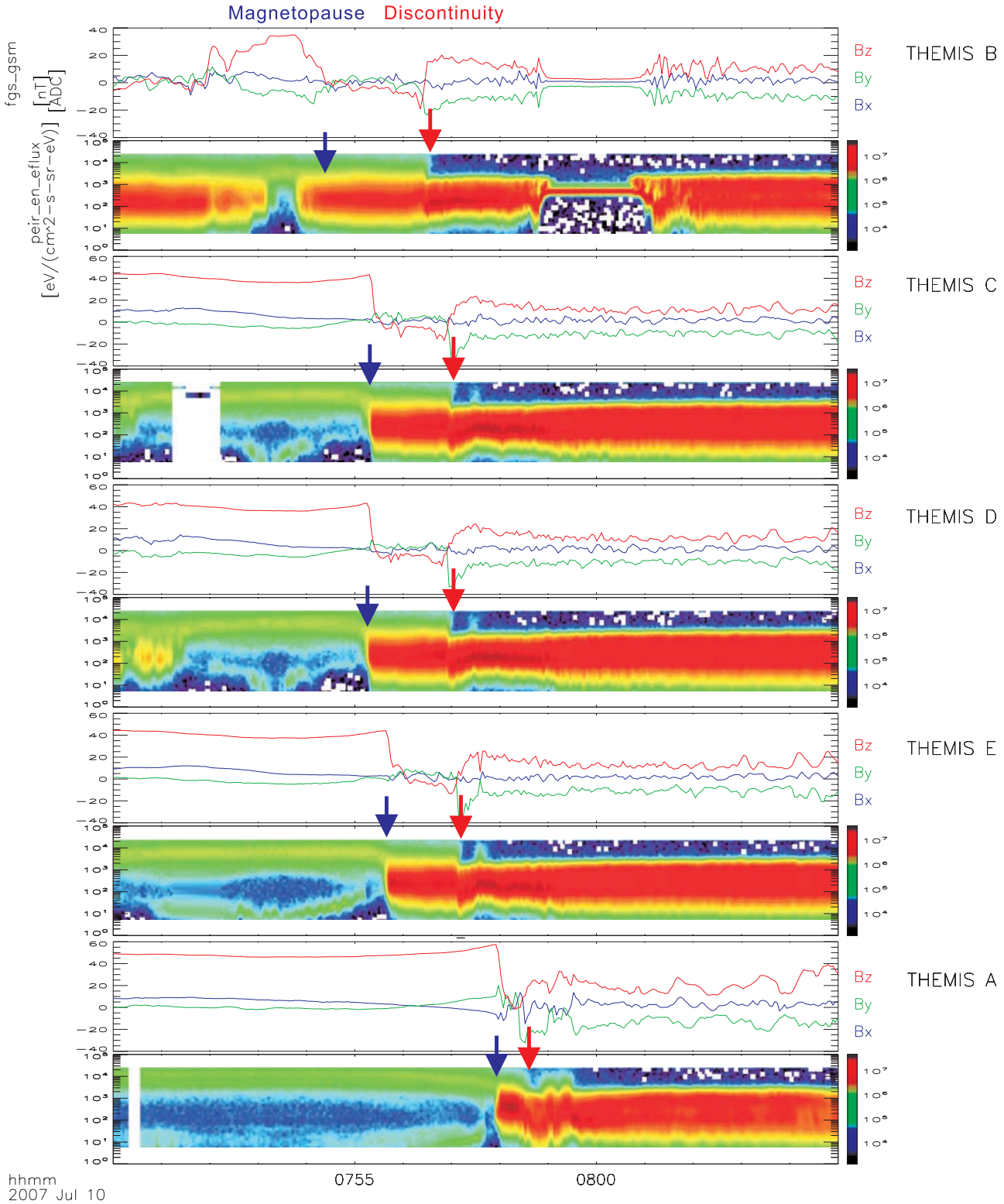

Figure 4. The magnetopause and discontinuity observed by all five THEMIS probes. The top panels show the magnetic field components and the ion spectrum from THEMIS B. The following panels show the same parameters from THEMIS C, D, E and A, respectively. The blue and red arrows mark the magnetopause and discontinuity crossings, respectively.

tenuous ($n \sim 0.2$ cm^{-3}) while it is cold ($T \sim 150$ eV) and dense ($n \sim 20$ cm^{-3}) in the magnetosheath. The bow shock crossing at 1106 UT (marked by a vertical dashed line) is also clearly associated with sharp changes in magnetic field and plasma parameters. Upstream is unshocked solar wind ($n \sim 5$ cm^{-3}, $|V_x| \sim 300$ km/s) and downstream is magnetosheath plasma (n ~ 20 cm^{-3}, $|V_x| < 100$ km/s). The most interesting time interval (from 0745 UT to 0815 UT,

Table 2. Magnetopause Crossing[a]

Probe	UT	Position in GSE (R_E)	Normal (GSE) (MVA)	V_x (km/s)
B	07:54:24	(12.26, 0.51, −3.32)	(0.985, −0.077, −0.153)	
C, D	07:55:18	(11.86, 0.16, −3.19)	(0.998, 0.052, −0.046)	−47.2
E	07:55:38	(11.72, 0.14, −3.17)	(0.990, −0.115, −0.083)	−44.6
A	07:57:53	(10.68, −0.80, −2.77)	(0.994, 0.091, 0.062)	−49.1

[a]Marked by blue arrows in Figure 4.

shaded region) is seen with greater time resolution in Figure 3.

[9] From 0753 UT to 0754 UT, THEMIS B was in the dayside magnetosphere which can be clearly seen from the low plasma ion density (second panel in Figure 3), high temperature (third panel), and ion and electron spectrum (last two panels). The two magnetopause crossings are marked by blue dashed lines and the normal directions obtained from Minimum Variance Analysis (MVA) method are shown in Table 1. The normal directions of these two magnetopauses are consistent with that of the first magnetopause crossing at 0550 UT (marked by a black dashed line in Figure 2) suggesting that the magnetopause was not greatly deformed.

[10] At 07:56:34, THEMIS B crossed a discontinuity (marked by a red dashed line in Figure 3) which is characterized by a change in the magnetic field direction and plasma ion density. It is interesting that features of the ion spectrum on the left hand side of the discontinuity are different from those on the right hand side. THEMIS B observes more suprathermal (>3 keV) ions before than after the discontinuity.

[11] At 0759 UT, THEMIS B crossed the bow shock (marked by a black dashed line in Figure 3) and stayed in the solar wind for 2 min. Then THEMIS B crossed the bow shock again at 0801 UT and returned to the magnetosheath. The bow shock therefore moved earthward and then sunward. It is interesting to note that the time between the consecutive magnetopause, discontinuity and first bow shock crossing is only 5 min.

[12] The magnetopause and discontinuity crossings have been observed by all 5 THEMIS probes. Figure 4 shows the magnetic field components and the ion spectrum from all 5 THEMIS probes. The blue and red arrows mark the magnetopause and discontinuity crossings, respectively. The velocity of the magnetopause and discontinuity motion can be obtained by timing analysis based on multispacecraft observations of the same structure. The results are shown in Tables 2 and 3. The velocities are obtained using consecutive probe pairs, i.e., B and C/D (C and D are very close to each other); C/D and E; E and A. The velocities of the magnetopause motion are −47.2 km/s, −44.6 km/s and −49.1 km/s with an average of −47 km/s. The minus signs indicate the magnetopause is moving earthward. The velocities of the discontinuity motion are −89.8 km/s, −89.2 km/s and −78.9 km/s with an average of −86 km/s. There is a trend that the discontinuity decelerates as it propagates toward the magnetopause. Since only THEMIS B observed the bow shock crossing, multispacecraft timing analysis can not be applied to calculate the velocity of the bow shock motion. However, the average velocity of the bow shock can be estimated assuming it was located at 13.5 R_E (the position observed by THEMIS B at 1106 UT, see Figure 2) before its interaction with the interplanetary shock. It took the discontinuity 85 s to propagate from the original bow shock location 13.5 R_E to 12.3 R_E. THEMIS B observed the bow shock crossing 150 s after the discontinuity passage, so it took the bow shock 235 s to move from 13.5 R_E to 12.3 R_E. The velocity of the bow shock motion is (12.3 R_E−13.5 R_E)/235 s = −33 km/s. The bow shock speed of 33 km/s is the lower limit because the solar wind dynamic pressure before the interaction of the bow shock and the interplanetary shock is smaller than that at 1106 UT (1.1 nPa <1.4 nPa, see the first panel in Figure 7).

[13] The detailed structure of the discontinuity is shown in Figure 5. It is characterized by increases in the magnitude of the magnetic field and plasma density and a decrease in the plasma ion temperature.

3. Discussion

3.1. Shock-Shock Interaction

[14] The characteristics of the discontinuity observed by the THEMIS spacecraft are very similar to those expected for new discontinuities produced by the interaction of interplanetary and bow shocks [*Samsonov et al.*, 2006; *Šafránková et al.*, 2007; *Přech et al.*, 2008] in the sense that the total magnetic field and density increase and the temperature decreases. The inward and outward motion of the bow shock is also consistent with simulations and observations of shock-shock interactions [*Samsonov et al.*, 2006; *Šafránková et al.*, 2007]. We checked the upstream solar wind observations for evidence of an interplanetary shock which might have driven the bow shock and magnetopause motion. The magnetic field features of the discontinuity were used to identify the interplanetary shock since the rotation of the field in the sheath should be similar to that upstream.

[15] We checked upstream solar wind observations from both ACE and WIND spacecraft which were located at around (225, −10, 20) GSE R_E and (260, −50, 17) GSE R_E, respectively. Unfortunately neither spacecraft is a good solar wind monitor for the whole time interval from 0550 UT to 1106 UT when THEMIS B was mainly in the magnetosheath. The ACE spacecraft is a good solar wind monitor from 0835 UT to 1106 UT which can be seen from the clock angle comparison in the second panel of Figure 2. However, ACE did not observe any discontinuities with similar rotation of the magnetic field to that observed by THEMIS B near 0757 UT. On the other hand, the WIND spacecraft is a good solar wind monitor from 0720 UT to 0930 UT. (The time shift of 110 min has been used to achieve the best match in the magnetic field features of WIND and THEMIS observations.) Therefore for the time interval of interest (0754 UT to 0801 UT), the WIND spacecraft is a good solar

Table 3. Discontinuity Crossing[a]

Probe	UT	Position in GSE (R_E)	Normal (GSE) (MVA)	V_x (km/s)
B	07:56:34	(12.29, 0.53, −3.33)	(0.999, −0.036, 0.016)	
C, D	07:57:03	(11.88,0.17,−3.20)	(0.993, −0.084, −0.089)	−89.8
E	07:57:13	(11.74,0.15,−3.17)	(0.988, −0.112, −0.110)	−89.2
A	07:58:37	(10.70,−0.79,−2.77)	(0.956, 0.075, 0.282)	−78.9

[a]Marked by red arrows in Figure 4.

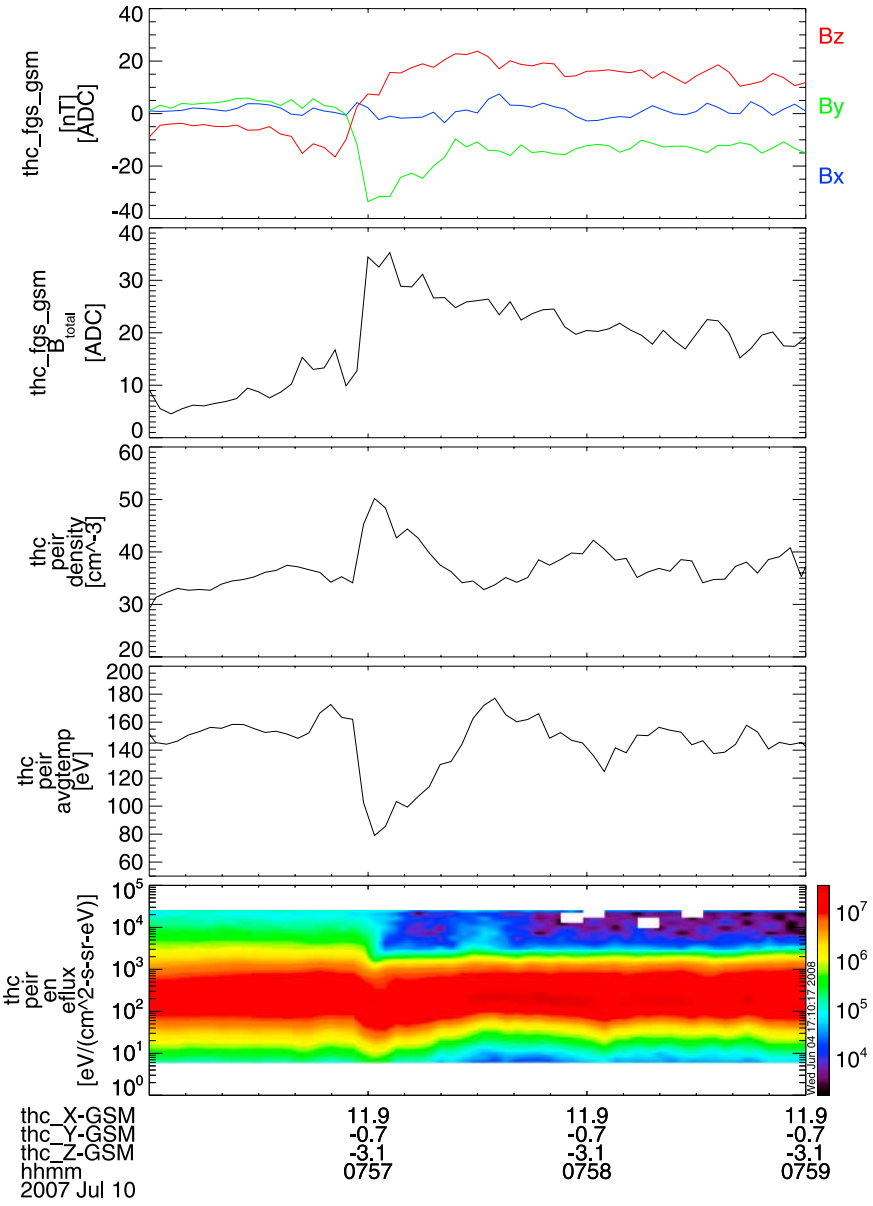

Figure 5. The discontinuity observed by THEMIS C. From the top, the panels show components of the magnetic field, magnitude of the magnetic field, plasma ion density, temperature and spectrum.

wind monitor and it did observe an interplanetary shock with similar rotation of the magnetic field to that observed by the THEMIS spacecraft.

[16] Figure 6 shows an interplanetary shock observed by the WIND spacecraft upstream at (260, −50, 17) R_E in GSE coordinate system. The top four panels show plasma moments from 3D PLASMA Analyzer [*Lin et al.*, 1995] and the bottom two panels show MFI [*Lepping et al.*, 1995] magnetic fields. It is noted that the proton density measured by WIND 3DP is different from that measured by SWE instrument (not shown). Following A. Szabo's suggestion, we rescaled the 3DP data to the SWE average values by adding 3.5 #/cm^3 when doing shock parameter calculations. The vertical dashed red line at 0608 UT marked the interplanetary shock crossing. The B_y component changed from ∼0 to negative and the B_z component changed from ∼0 to positive across the shock. The rotation of the magnetic field across this interplanetary shock matches that of the discontinuity observed THEMIS spacecraft very well (compare the first panel in Figure 3 and the fifth panel in Figure 6). The B_x component observed by WIND is large and nearly zero when observed by THEMIS. The difference in B_x component is due to the field line draping in the magnetosheath. The interplanetary shock is characterized by increases in solar wind density, temperature, velocity and the magnitude of the magnetic field. Parameters of the interplanetary shock have been calculated using Shock and Discontinuities Analysis Tool (SDAT) [*Viñas and Holland*, 2005] which uses the Viñas-Scudder analysis method [*Viñas and Scudder*, 1986] based on the Rankine-Hugoniot conservation equations. The shock parameters are summarized in Table 4. The shock is a weak fast forward shock with Alfvén Mach number M_A = 1.4. It is noted that during this time interval, the solar wind is very cold (3 eV) and slow (310 km/s).

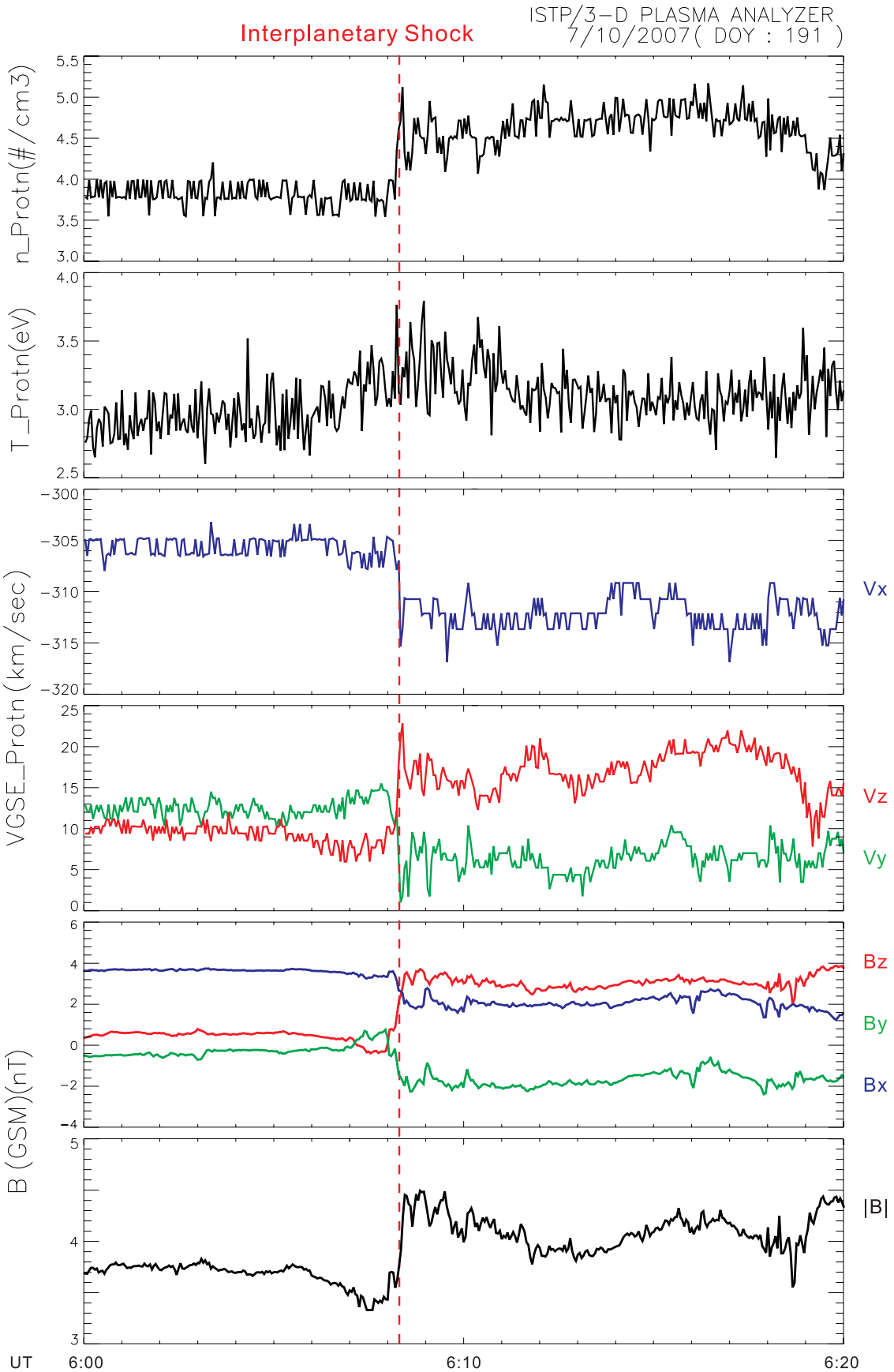

Figure 6. WIND 3D PLASMA and MFI observations of an interplanetary shock passage. From the top, the panels show the solar wind density, temperature, components of the solar velocity, components of IMF and the magnitude of the IMF. The interplanetary shock is marked by the vertical red dashed line.

Table 4. Parameters of the Interplanetary Shock

Parameter	Value	Standard Deviation
Normal (in GSE)	(0.93, −0.37, −0.09)	
θ_{Bn} (deg)	20.0	5.4
Shock velocity along shock-normal direction (km/s)	−330	12
Sound speed (km/s)	0.284	0.008
Alfven speed (km/s)	30.072	0.277
Magnetosonic Mach number	1.374	0.030
Alfven Mach number	1.374	0.030

[17] The ACE spacecraft missed the interplanetary shock observed by the WIND spacecraft might be due to the fact that the shock has a limited dimension in *y* direction (less than the separation of ACE and WIND). Also, the low-Mach number interplanetary shocks may evolve on their way to the Earth, usual planarity assumption may not be satisfied and the interplanetary shocks may not be homogeneous along their fronts.

[18] Previous studies show that the interaction of an interplanetary shock with the bow shock launches a fast shock into the magnetosheath and form a new discontinuity [*Zhuang et al.*, 1981] where the magnetic field strength and density

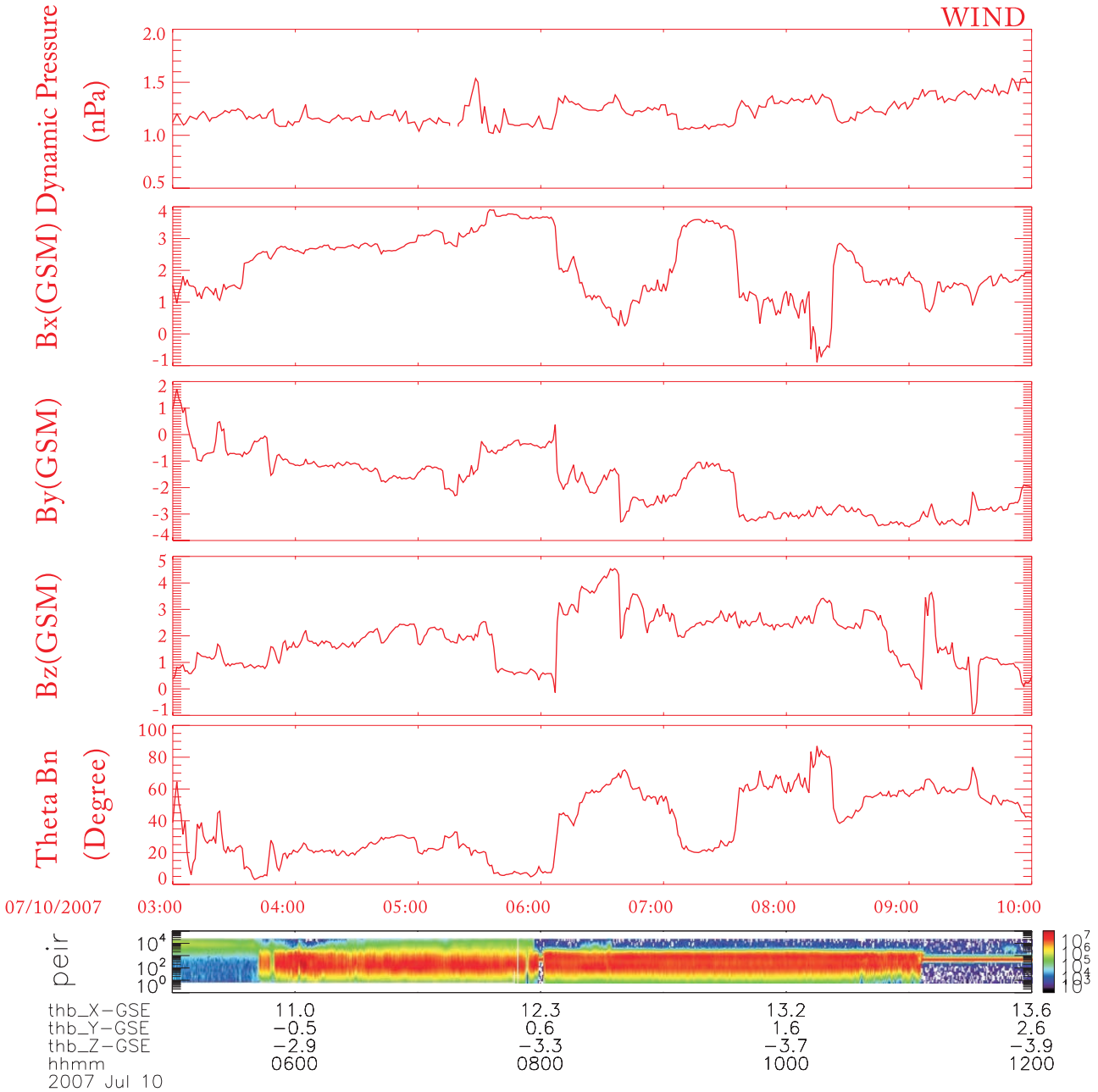

Figure 7. The solar wind dynamic pressure and the IMF observed by the WIND spacecraft together with the ion spectrum from THEMIS from 0500 UT to 1200 UT on 10 July 2007. The first panel shows the solar wind dynamic pressure, and the following three panels show components of the IMF in GSM coordinates. The fifth panel shows the angle between the IMF direction and the bow shock normal.

increase, the temperature decreases and the velocity remains unchanged [*Samsonov et al.*, 2006; *Šafránková et al.*, 2007; *Přech et al.*, 2008]. However, in the event presented here no fast shock has been observed. Instead, the transmitted interplanetary shock took the form of a discontinuity where total magnetic field and density increase and the temperature decreases. The rotation of the magnetic field across this discontinuity was similar to that of the interplanetary shock. The difference is possibly due to the fact that the interplanetary shock is very weak and the transmitted fast shock velocity is very close to the discontinuity behind it so their features are combined to form a new discontinuity. MHD simulations may help to understand the weak shock-bow shock interaction better.

3.2. Ion Acceleration

[19] It is interesting that the features of ion spectrum on the left hand side of the discontinuity are different from those on the right hand side. THEMIS B observes more suprathermal (>3 keV) ions before than after the discontinuity at 0757 UT. Figure 7 shows the solar wind dynamic pressure and the IMF observed by the WIND spacecraft together with the ion spectrum from THEMIS B. The first panel shows the solar wind dynamic pressure and the following three panels show components of the IMF in GSM coordinates. The fifth panel shows the angle between the IMF direction and the bow shock normal where the bow shock normal is in (0.956, −0.142, 0.256)GSE direction (determined from THEMIS B observation at 1106 UT). Prior to (after) the discontinuity, the bow shock is quasi-parallel (quasi-perpendicular). Since quasi-parallel shocks are believed to be the best sites for Fermi acceleration [*Burgess*, 2007], it is not surprising that there are more higher energy (>3 keV) ions when the bow shock is a quasi-parallel shock.

3.3. Magnetopause Motion

[20] The sudden magnetopause inward movement is observed by THEMIS B, C, D and E prior the THEMIS B discontinuity first registration, therefore the motion is unlikely due to the impact of the discontinuity. We checked the solar wind monitor for features which might have driven the magnetopause motion. We do see changes in the solar wind parameters at around 06:06:45 UT (Figure 6). Both the proton density and the velocity V_x component therefore the dynamic pressure increased slightly which could drive the earthward motion of the magnetopause. Meanwhile, there is a ∼17 degree change (θ_{Bn} changed from 18 degree to 35 degree) in the IMF orientation at 06:06:45 UT. Previous work suggested that the fraction of the solar wind dynamic pressure applied to the magnetosphere depends upon the orientation of the IMF and even a small change in the IMF orientation can change the pressure significantly [e.g., *Fairfield et al.*, 1990]. When the IMF is radial (transverse to the Sun-Earth line), the pressure applied to the magnetosphere is smaller (higher). In the event presented here, θ_{Bn} increased from 18 degree to 35 degree which means the pressure applied to the magnetosphere would increase and could have driven the earthward motion of the magnetopause.

4. Conclusions

[21] In this paper, we present an observational study of the dynamic motion of the bow shock and the magnetopause and suggest that the dynamic motion and the discontinuity results from the interaction of an interplanetary shock with the Earth's bow shock. Timing analysis shows that the magnetopause and the discontinuity were moving earthward with average speeds of ∼47 km/s and ∼90 km/s, respectively. There is a trend that the discontinuity decelerates as it propagates toward the magnetopause. After the interaction, the transmitted interplanetary shock took the form of a discontinuity where total magnetic field and density increase and the temperature decreases. The rotation of the magnetic field across this discontinuity was similar to that of the interplanetary shock. The expected fast shock ahead of the discontinuity for shock-shock interaction was not observed.

[22] **Acknowledgments.** We acknowledge NASA contract NAS5-02099 and V. Angelopoulos for use of data from the THEMIS mission. Special thanks to Adolfo F. Viñas for providing the SDAT to calculate the shock parameters. Thanks to Adam Szabo for his advice on using WIND 3DP data.

[23] Zuyin Pu thanks the reviewers for their assistance in evaluating this paper.

References

Angelopoulos, V. (2008), The THEMIS mission, *Space Sci. Rev.*, *47*, doi:10.1007/s11214-008-9336-1.

Auster, H. U., et al. (2008), The THEMIS fluxgate magnetometer, *Space Sci. Rev.*, *73*, doi:10.1007/s11214-008-9365-9.

Belcher, J. W., and L. Davis Jr. (1971), Large-amplitude Alfvén waves in the interplanetary medium, 2, *J. Geophys. Res.*, *76*, 3534–3563.

Binsack, J. H., and V. M. Vasyliunas (1968), Simultaneous IMP 2 and OGO 1 observations of bow shock comression, *J. Geophys. Res.*, *73*, 429–433.

Burgess, D. (2007), Particle acceleration at the Earth's bow shock, in *Lecture Notes in Physics*, vol. 725, edited by K.-L. Klein and A. L. MacKinnon, pp. 161–191, Springer, Berlin.

Burlaga, L. F. (1971), Hydromagnetic waves and discontinuities in the solar wind, *Space Sci. Rev.*, *12*, 600–657.

Burlaga, L. F., and K. W. Ogilvie (1969), Causes of sudden commencements and sudden impulses, *J. Geophys. Res.*, *74*, 2815–2825.

Fairfield, D. H., W. Baumjohann, G. Paschmann, H. Luehr, and D. G. Sibeck (1990), Upstream pressure variations associated with the bow shock and their effects on the magnetosphere, *J. Geophys. Res.*, *95*, 3773–3786.

Formisano, V., and G. Mastrantonio (1975), On the Earth's bow shock motion and speed, *Space Sci. Rev.*, *17*, 781–786.

Formisano, V., P. C. Hedgecock, G. Moreno, F. Palmiotto, and J. K. Chao (1973), Solar wind interaction with the Earth's magnetic field: 2. Magnetohydrodynamic bow shock, *J. Geophys. Res.*, *78*, 3731–3744.

Glassmeier, K.-H., et al. (2008), Magnetospheric quasi-static response to the dynamic magnetosheath: A THEMIS case study, *Geophys. Res. Lett.*, *35*, L17S01, doi:10.1029/2008GL033469.

Gosling, J. T., J. R. Asbridge, S. J. Bame, A. J. Hundhausen, and I. B. Strong (1967), Measurements of the interplanetary solar wind during the large geomagnetic storm of April 17–18, 1965, *J. Geophys. Res.*, *72*, 1813.

Gosling, J. T., J. R. Ashbridge, S. J. Bame, A. J. Hundhausen, and I. B. Strong (1968), Satellite measurements of interplanetary shock waves, *Astron. J.*, *73*, 61.

Greenstadt, E. W., P. C. Hedgecock, and C. T. Russell (1972), Large-scale coherence and high velocities of the Earth's bow shock on February 12, 1969, *J. Geophys. Res.*, *77*, 1116–1122.

Grib, S. A., B. E. Briunelli, M. Dryer, and W.-W. Shen (1979), Interaction of interplanetary shock waves with the bow shock-magnetopause system, *J. Geophys. Res.*, *84*, 5907–5921.

Guha, J. K., D. L. Judge, and J. H. Marburger (1972), OGO 5 magnetic-field data near the Earth's bow shock: A correlation with theory, *J. Geophys. Res.*, *77*, 604–610.

Koval, A., J. Šafránková, Z. Němeček, and L. Přech (2006), Propagation of interplanetary shocks through the solar wind and magnetosheath, *Adv. Space Res.*, *38*, 552–558, doi:10.1016/j.asr.2006.05.023.

Lepidi, S., U. Villante, A. J. Lazarus, A. Szabo, and K. Paularena (1996), Observations of bow shock motion during times of variable solar wind conditions, *J. Geophys. Res.*, *101*, 11,107–11,124, doi:10.1029/96JA00478.

Lepping, R. P., et al. (1995), The Wind Magnetic Field Investigation, *Space Sci. Rev.*, *71*, 207–229, doi:10.1007/BF00751330.

Lin, R. P., et al. (1995), A three-dimensional plasma and energetic particle investigation for the Wind spacecraft, *Space Sci. Rev.*, *71*, 125–153, doi:10.1007/BF00751328.

Maksimovic, M., S. D. Bale, T. S. Horbury, and M. André (2003), Bow shock motions observed with CLUSTER, *Geophys. Res. Lett.*, *30*(7), 1393, doi:10.1029/2002GL016761.

Maynard, N. C., W. J. Burke, D. M. Ober, C. J. Farrugia, H. Kucharek, M. Lester, F. S. Mozer, C. T. Russell, and K. D. Siebert (2007), Interaction of the bow shock with a tangential discontinuity and solar wind density decrease: Observations of predicted fast mode waves and magnetosheath merging, *J. Geophys. Res.*, *112*, A12219, doi:10.1029/2007JA012293.

McFadden, J. P., C. W. Carlson, D. Larson, M. Ludlam, R. Abiad, B. Elliott, P. Turin, M. Marckwordt, and V. Angelopoulos (2008), The THEMIS ESA plasma instrument and in-flight calibration, *Space Sci. Rev.*, *141*, 277–302, doi:10.1007/s11214-008-9440-2.

Ogilvie, K. W., and L. F. Burlaga (1969), Hydromagnetic shocks in the solar wind, *Sol. Phys.*, *8*, 422–434, doi:10.1007/BF00155390.

Přech, L., Z. Němeček, and J. Šafránková (2008), Response of magnetospheric boundaries to the interplanetary shock: Themis contribution, *Geophys. Res. Lett.*, *35*, L17S02, doi:10.1029/2008GL033593.

Šafránková, J., Z. Němeček, L. Přech, A. A. Samsonov, A. Koval, and K. Andréeová (2007), Modification of interplanetary shocks near the bow shock and through the magnetosheath, *J. Geophys. Res.*, *112*, A08212, doi:10.1029/2007JA012503.

Samsonov, A. A., Z. Němeček, and J. Safránková (2006), Numerical MHD modeling of propagation of interplanetary shock through the magnetosheath, *J. Geophys. Res.*, *111*, A08210, doi:10.1029/2005JA011537.

Samsonov, A. A., D. G. Sibeck, and J. Imber (2007), MHD simulation for the interaction of an interplanetary shock with the Earth's magnetosphere, *J. Geophys. Res.*, *112*, A12220, doi:10.1029/2007JA012627.

Sari, J. W., and N. F. Ness (1969), Power spectra of the interplanetary magnetic field, *Sol. Phys.*, *8*, 155–165, doi:10.1007/BF00150667.

Shen, W.-W., and M. Dryer (1972), Magnetohydrodynamic theory for the interaction of an interplanetary double-shock ensemble with the Earth's bow shock, *J. Geophys. Res.*, *77*, 4627–4644.

Smith, C. W., J. L'Heureux, N. F. Ness, M. H. Acuña, L. F. Burlaga, and J. Scheifele (1998), The ACE Magnetic Fields Experiment, *Space Sci. Rev.*, *86*, 613–632, doi:10.1023/A:1005092216668.

Spreiter, J. R., A. L. Summers, and A. Y. Alksne (1966), Hydromagnetic flow around the magnetosphere, *Planet. Space Sci.*, *14*, 223.

Viñas, A. F., and M. P. Holland (2005), Shock and Discontinuities Analysis Tool (SDAT), *Eos Trans. AGU*, *86*(18), Jt. Assem. Suppl., Abstract SH51B-10.

Viñas, A. F., and J. D. Scudder (1986), Fast and optimal solution to the 'Rankine-Hugoniot problem,' *J. Geophys. Res.*, *91*, 39–58.

Völk, H. J., and R.-D. Auer (1974), Motions of the bow shock induced by interplanetary disturbances, *J. Geophys. Res.*, *79*, 40–48.

Wu, B.-H., M. E. Mandt, L. C. Lee, and J. K. Chao (1993), Magnetospheric response to solar wind dynamic pressure variations: Interaction of interplanetary tangential discontinuities with the bow shock, *J. Geophys. Res.*, *98*, 21,297.

Zastenker, G. N., V. N. Smirnov, C. T. Russell, H. S. Bridge, and A. Lazarus (1988), Bow shock motion with two-point observations - Prognoz 7, 8 and ISEE 1, 2; Prognoz 10 and IMP 8, *Adv. Space Res.*, *8*, 171–174, doi:10.1016/0273-1177 (88)90128-7.

Zhuang, H. C., C. T. Russell, E. J. Smith, and J. T. Gosling (1981), Three-dimensional interaction of interplanetary shock waves with the bow shock and magnetopause: A comparison of theory with ISEE observations, *J. Geophys. Res.*, *86*, 5590–5600.

T. A. Fritz, Center for Space Physics, Boston University, Boston, MA 02215, USA.

K.-H. Glassmeier, Institute for Geophysics and Extraterrestrial Physics, Technical University of Braunschweig, D-38106 Braunschweig, Germany.

D. Larson and J. P. McFadden, Space Sciences Laboratory, University of California, Berkeley, CA 94720, USA.

D. G. Sibeck and H. Zhang, NASA Goddard Space Flight Center, Greenbelt, MD 20771, USA. (hzhang@helio.gsfc.nasa.gov)

Q.-G. Zong, Center for Atmospheric Research, University of Massachusetts Lowell, Lowell, MA 01854, USA.